

## **LINEAR INDUCTION MOTOR THRUST FORCE REDUCTION DUE TO END EFFECTS FOR VARIOUS AIR GAP WIDTHS AND FEM CALCULATIONS**

**A.H. Selcuk**

*Department of Electrical and Electronics Engineering, Balikesir University, Balikesir, Turkey, aselcuk@balikesir.edu.tr*

**Abstract-** The air gap width has a significant influence on the magnitude of magnetic flux density in an electrical machine. As the air gap width decreases, the magnetic field becomes higher. However, linear motors (LIM) have end effects due to the sharp endings at both sides of the machine. As the rotor enters into or leaves from the magnetic field, a reaction occurs as breaking, which is called end effect. End effects change with speed of the motor and strength of the magnetic field. Reducing the air gap width causes higher magnetic field. But this makes end effects become more significant, especially at high speeds. This work uses finite element method (FEM) to calculate force reductions and presents them as graphics for a simplified short primary LIM model due to end effects. To build a reference, a very long model having the same parameters is built which is supposed to have no end effects. The results of the original motor model are then compared with the longer reference model's. This work helps build a basis to understand and interpret the influence of end effects on the thrust force with the variation of the air gap. The goodness equation is also defined again introducing an end effect factor for LIMs.

**Keywords:** Computational Electromagnetics, End Effect, Electromagnetic Analysis, FEM, LIM.

### **I. INTRODUCTION**

Linear electrical machines can be obtained (or supposed to be obtained) by cutting a rotating motor in radial direction until its axis and then opening it to form a straight line. The machine obtained by this way has the same principles of motion with the original rotating machine. All types of rotating machines can also be constructed as linear machines theoretically.

It is possible to build a linear machine as a generator or a rotor. Since the usage of linear motors eliminates the need for additional mechanisms like gearbox to transform the rotation into linear motion, they are preferred instead of rotating motors in many applications requiring linear motion. One of the linear motor types is linear induction motor that is widely used especially in magnetic trains. By means of the linear motion system of a magnetic train, it is possible to levitate and move the train simultaneously. The usage of linear motors varies from high speed trains to biomedical devices.

Despite its great advantage of direct linear motion, a linear induction motor has a disadvantage called *end effect* (especially longitudinal end effect) which is not valid or present in a rotating motor. End effects can be considered as a disadvantage of linear machines.

Mainly, the types of end effects in the direction of movement of a LIM can be written as [1]:

- Static longitudinal end effects
- Speed dependent longitudinal end effects

Linear motors are of mainly two types as short primary and short secondary motors. If the rotor (secondary) is very long (i.e. infinitely long) and stator (the part of the motor having excitation windings) is of limited length, then it is called a short primary linear motor. If the primary (stator) is very (infinitely) long and secondary is short as compared with the primary, then it is a short secondary linear motor. Short primary linear induction motors are more influenced by the end effects than short secondary motors [2].

In speaking the performance of an electrical motor, some concepts must be cleared. How should we describe the "performance"? How can one talk about the goodness of a machine? What are the design constraints and tolerances? Cannot we use a larger motor instead of examining end effects?

The goodness of a machine is defined by [2] as:

$$G = \frac{\sigma\mu\omega A_e A_m}{l_e l_m} \quad (1)$$

where, the indices *e* and *m* refer to electrical and magnetic circuits, *A* and *l* refer to the area and length,  $\omega$ ,  $\sigma$  and  $\mu$  are the angular frequency, electrical conductance and magnetic permeability, respectively.

According to this equation, as the air gap width (which refers to  $l_m$ ) decreases, the machine gets better. However, as the gap gets narrower, the influences of the end effects become more significant. Since the longitudinal end effects are speed dependent, a speed dependent end effect factor  $E_l(v)$  may be introduced into the equation for linear machines. Then the equation becomes:

$$G = \frac{\sigma\mu\omega A_e A_m}{l_e l_m} E_l(v) \quad (2)$$

In a linear induction motor, end effects cause a reduction in the thrust force. As a result of this, they cause to lower the synchronous speed, if the synchronous speed is defined as the speed at which an induction motor produces zero torque or thrust force. All the variations of thrust force and synchronous speed with respect to the air gap width are given as graphics throughout the text.

The double sided short primary linear induction motor explained in [1] is modeled in 2D and a current sheet is placed in the stator as excitation instead of wires, so that the current density distribution is an ideal sinusoidal. This is done to obtain and understand the influences of end effects in an ideal manner.

End effects have been investigated with various methods. Gieras et al. have taken end effects into account by using additional parameters or equations in equivalent circuit of induction motor [3]. They considered the air gap field as a sum of two fields. One of them is the main travelling wave and the other one is an attenuating wave of end effects. The same approach has been used by Sung to perform vector control of LIM [4]. Using FEM with the help of a thrust correction coefficient, Kwon et al. have taken into account the end effects of a LIM [5]. A rotating magnet was designed and calculated with FEM in order to compensate end effects of LIM by Fujii and Harada [6]. They reported that the thrust of the LIM with the compensator was the same as if it had no end effects.

With the help of FEM, a d-q axis transient model for simulation has been evaluated [7]. The asymmetric d-q equivalent constants for static and dynamic end effects have been determined. LIMs can also be used as accelerating devices such as coil guns. To perform electromagnetic launching, tubular linear induction motors (TLIM) have been investigated and constructed [8]. Polzin et al. optimized the energy transfer in coil-guns by using dynamic impedance parameter [9].

The usage of the LIMs in transportation systems is especially important. Morizane et al. [10] have proposed a new control method for maglev transportation systems to control acceleration and levitation of the LIM simultaneously and separately without using another system for levitation. They have driven the levitating component of the force by another source having the synchronous frequency with the instantaneous speed, which had no effect on the traction force.

Amiri and Mendrela have suggested a new model for LIMs, when the excitation frequency of the equivalent circuit is constant [11]. They have introduced new branches into the equivalent circuit to express static and dynamic end effects separately. They have used Duncan model to obtain the speed dependent end effects and modified for the saturation of iron. The results have then been compared with FEM simulation's.

Jang et al. have investigated the dynamic characteristics of linear motor used in the levitation vehicles. After using equivalent circuit to predict the motor performance with simulation, they have compared

the results with finite element method [12]. Zhang et al. have proposed to use a vector electric potential to analyze transverse edge effects of a LIM [13]. In [13], a novel maglev transportation platform having two subsystems for levitation and propulsion has been developed and optimized with the help of finite element analysis.

Duan et al. designed a precision linear positioning device having two subsystems for levitation and propulsion. In order to optimize the electromagnet distribution, they have used finite element method [14].

In this work, with the help of 2D FEM, a data basis is built to help better understanding and interpreting of the longitudinal end effects of a LIM from the thrust force point of view. The air gap width is changed from 0.5 mm to 5 mm while the speed of the rotor is taken from 0 to 12-14 m/s, at which the synchronous speed changes from 12.3 to 13.5 m/s because of end effects.

**II. ACTUAL MOTOR AND ITS SIMPLIFIED MODEL**

The actual motor is modelled in Firat University, Elazig, Turkey and force values are evaluated by the finite element method. The actual linear motor has a massive disk of steel as its rotor (Figure 1). An adjustable air gap, two sided stator makes the rotor rotate. The stator has a 56 cm length, 4 cm width and 36 slots. It consists of 434 silicon coated plates each having 0.3 mm width. It is of two parts of width 130 mm. The depth of the slots is 18 mm with the width of 8 mm. Each part of the stator consists of 36 slots. The motor is excited by three phases each having 4 coils. Coils have sub coils which are not of equal width and equal pitch. The pitch values of the sub coils are 6.8 and 10 slots. Every sub coil has 22 couples of windings. The conductors of the windings have the diameter of 3×0.65 mm [1].

The intersection of stator is shown in Figure 2. To simplify the model, current sheet in Figure 3 is used. Because of the symmetry of the double sided short primary linear motor, the half of the complete region of solution can be used. This reduces the computation time. Figure 3 also shows the axis of symmetry at the top.

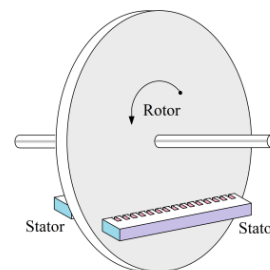


Figure 1. The linear induction motor at the laboratory [1]

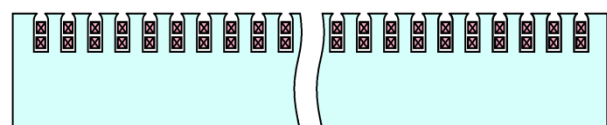


Figure 2. The side view of the stator [1]

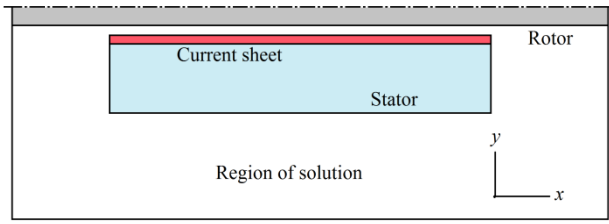


Figure 3. The region of solution used for the finite element method [1]

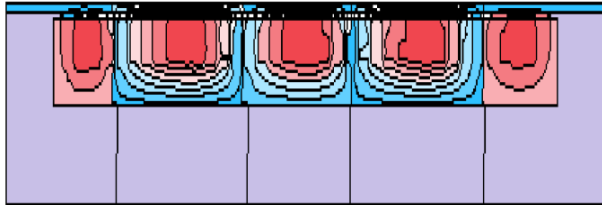


Figure 4. Finite element calculation equipotential lines ( $B$  lines)

The usage of the current sheet provides a perfect sinusoidal current distribution which is useful in theoretical understanding of the phenomenon. Figure 4 shows equipotential lines (which are also flux density lines) as the result of the calculation.

### III. METHOD OF FORCE CALCULATIONS

After calculating the magnetic vector potential values with finite element method, the magnetic flux density values on each rotor element are found by Equation (3) [15, 16].

$$B_x = -\frac{\partial A}{\partial y}, B_y = \frac{\partial A}{\partial x} \quad (3)$$

in both directions, where,  $A$  is the magnitude of the vector potential in  $z$  direction. In 2D FEM analysis it has only one component. Since (refer to Figure 5) [15,16]:

$$A = A_0N_0 + A_1N_1 + A_2N_2 \quad (4)$$

$$N_i = (a_i + b_i x + c_i y) / 2\Delta \quad (5)$$

then

$$B_x = (A_0c_0 + A_1c_1 + A_2c_2) / 2\Delta \quad (6)$$

$$B_y = (-A_0b_0 - A_1b_1 - A_2b_2) / 2\Delta \quad (7)$$

where,  $N_i$ s are called the shape functions and

$$a_0 = x_1y_2 - x_2y_1, a_1 = x_2y_0 - x_0y_2, a_2 = x_0y_1 - x_1y_0 \quad (8)$$

$$b_0 = y_0 - y_2, b_1 = y_2 - y_0, b_2 = y_0 - y_1 \quad (9)$$

$$c_0 = x_2 - x_1, c_1 = x_0 - x_2, c_2 = x_1 - x_0 \quad (10)$$

where,  $x_i$  and  $y_i$  are the coordinates of the  $i$ th corner and  $A_i$ s are the magnetic vector potential values at the corners of the triangle element.

The induced current density inside a rotor element is [16]:

$$J_e = \sigma(-j\omega A + vB_y) \quad (11)$$

$$J_e = -j\omega\sigma(A_0N_0 + A_1N_1 + A_2N_2) + v\sigma(-A_0b_0 - A_1b_1 - A_2b_2) / 2\Delta$$

where,  $\sigma$  stands for conductivity,  $\omega$  is the line angular frequency, and  $v$  is the speed of the rotor in  $x$  direction.

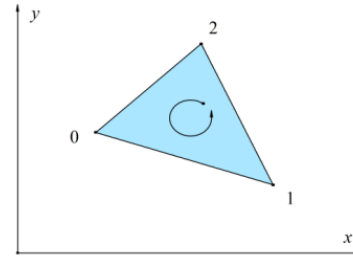


Figure 5. A triangular element of 2D FEM

Since the problem is assumed to be linear, integration gives the values of average current densities at the corner of the elements multiplied by the area of the element. Note that current density vector has only  $z$  component in 2D analysis.

FEM divides the region of solution into small elements which in our case triangularly shaped. On each element, the components of the force vector acting on the rotor elements can be calculated using the equations below [15, 16]:

$$F_x = \frac{1}{2} \text{Re} \left\{ \int_S J_e B_y^* ds \right\}, F_y = \frac{1}{2} \text{Re} \left\{ \int_S J_e B_x^* ds \right\} \quad (12)$$

and [16]

$$F_x = \frac{1}{2} \sigma \Delta \text{Re} \left\{ \left( vB_y - j\omega \frac{[A_0 + A_1 + A_2]}{3} \right) B_y^* \right\} \quad (13)$$

$$F_y = \frac{1}{2} \sigma \Delta \text{Re} \left\{ \left( vB_x - j\omega \frac{[A_0 + A_1 + A_2]}{3} \right) B_x^* \right\} \quad (14)$$

This calculation is repeated for every rotor element and summation gives the value of the total force. After summation of the contributions from all the elements, the value of the force is obtained.

Joule losses and air gap power are [15, 16]:

$$P_s = \frac{1}{2} \text{Re} \left\{ \int J_e E^* ds \right\} \quad (15)$$

in rotor elements and

$$P_g = \frac{1}{2} \text{Re} \left\{ \int E H^* ds \right\} \quad (16)$$

in air gap elements, respectively. These calculated values of power and force are the time average values.

### IV. FEM ANALYSIS RESULTS

The FEM calculations are made by using a computer program written by the author. The model is built by another program. Since the geometry of a linear motor is not so complicated, meshing process is rather simpler. After meshing the region of solution, data is given to the program. The program finds vector potential values at all the nodes of the mesh. Then it is possible to calculate magnetic flux densities, current density values and forces in the elements of the mesh. Summation of the force values on the rotor elements gives the total force value.

In order to compare the influence of edge effects, a very long model called X11 is built as a reference of comparison. This model is exactly same as the actual motor model except it is 11 times longer. The actual model is denoted as X1 model.

The program uses steady state analysis with the help of complex numbers. It is able to find the fields at particular rotor speeds. For each rotor speed, the calculation is repeated. The calculated force-speed graphics of X1 and X11 models are given in Figures 6-10.

The relatively small force values are because of the applied current. Since the analysis is linear, these relatively small values are out of question.

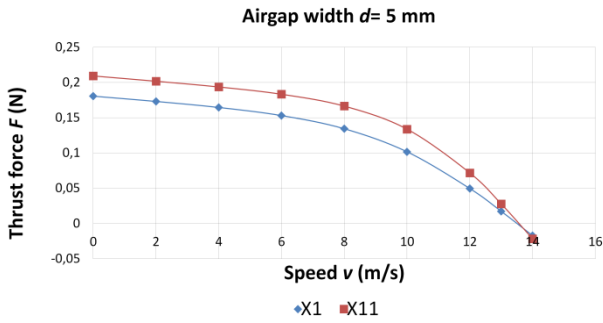


Figure 6. The force-speed characteristics of the LIM when  $d=5$  mm

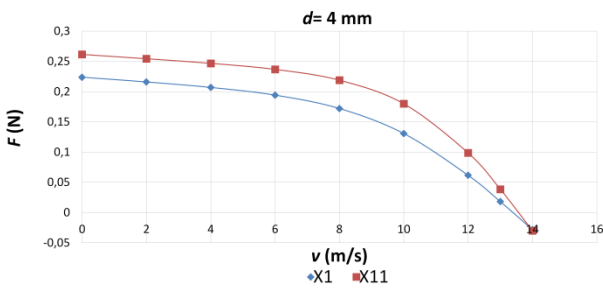


Figure 7. The force-speed characteristics of the LIM when  $d=4$  mm

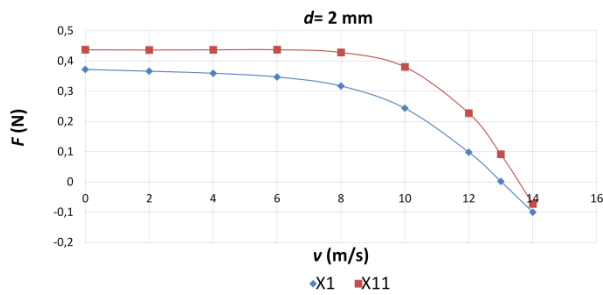


Figure 8. The force-speed characteristics of the LIM when  $d=2$  mm

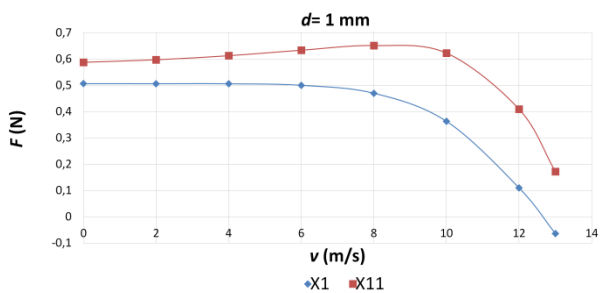


Figure 9. The force-speed characteristics of the LIM when  $d=1$  mm

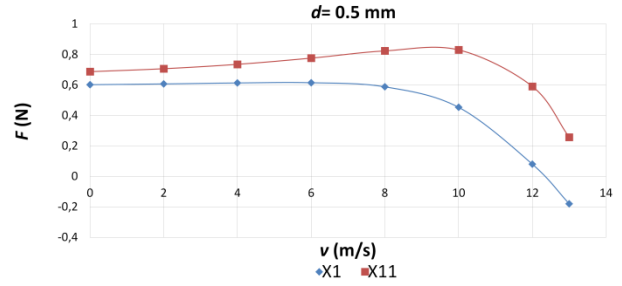


Figure 10. The force-speed characteristics of the LIM when  $d=0.5$  mm

The maximum thrust value for large air gap is at zero speed for this machine. As the air gap reduces, the maximum thrust value occurs at higher speeds. The maximum thrust point for X11 model changes with respect to the air gap width as expected. As the gap gets larger, the maximum thrust point gets closer to the zero speed. However, X1 model has a smaller variation. This must be because of breaking due to speed dependent end effects.

The synchronous speed decreases as the gap gets narrower, because the speed dependent end effects become more significant as the gap decreases. The rotor elements enter through and leave from a stronger magnetic field at the edges. The variation of the synchronous speed with respect to the air gap width is sketched in Figure 11.

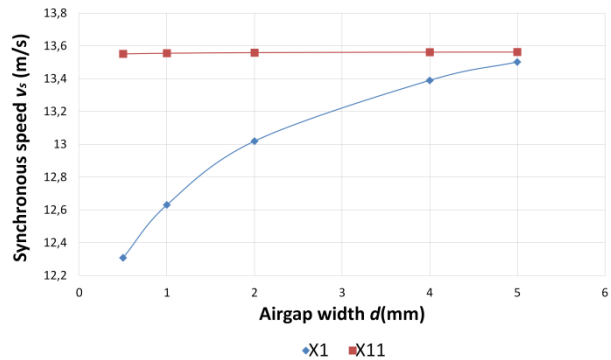


Figure 11. Variation of the synchronous speed with respect to air gap width

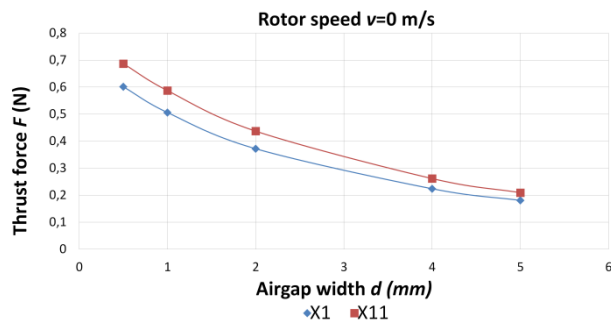


Figure 12. Variation of thrust force versus air gap width at rotor speed  $v=0$  m/s

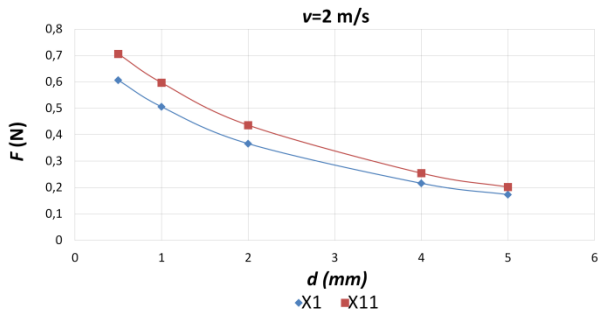


Figure 13. Variation of thrust force versus air gap width at rotor speed  $v=2$  m/s

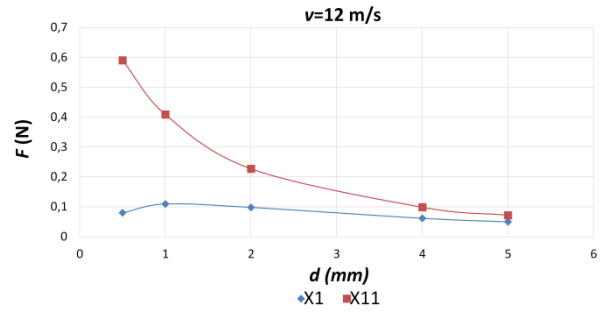


Figure 17. Variation of thrust force versus air gap width at rotor speed  $v=12$  m/s

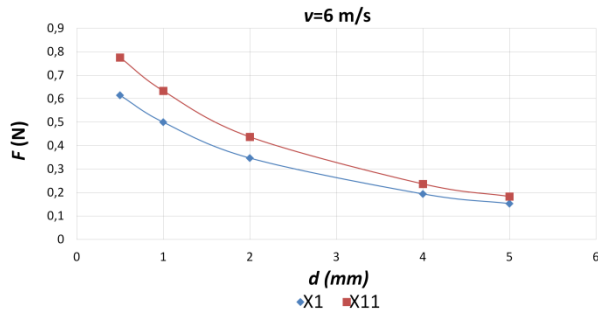


Figure 14. Variation of thrust force versus air gap width at rotor speed  $v=6$  m/s

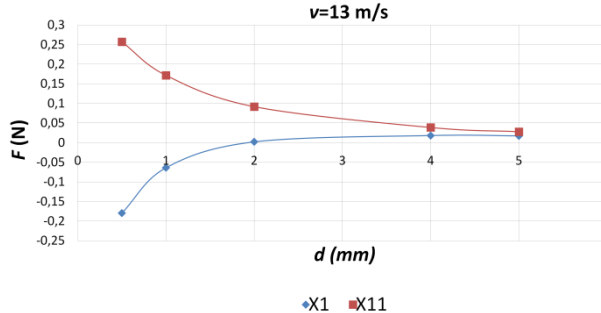


Figure 18. Variation of thrust force versus air gap width at rotor speed  $v=13$  m/s

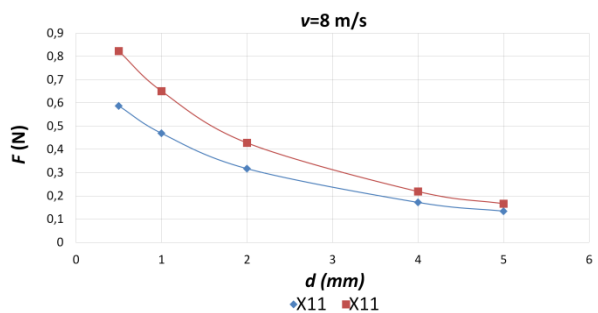


Figure 15. Variation of thrust force versus air gap width at rotor speed  $v=8$  m/s

In order to clarify the effect of speed on the end effects, it is better to express the thrust reduction in percentages. The Figure 19 shows this phenomenon.

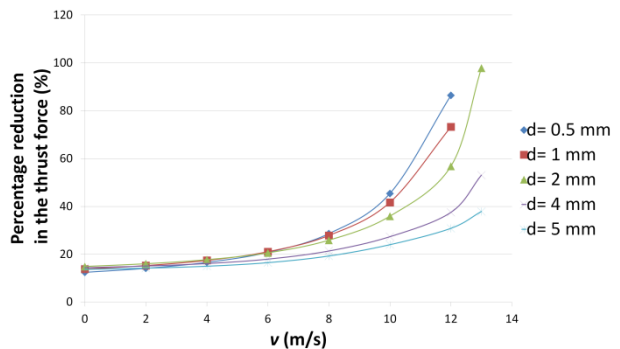


Figure 19. Percentage reduction of thrust force versus rotor speed

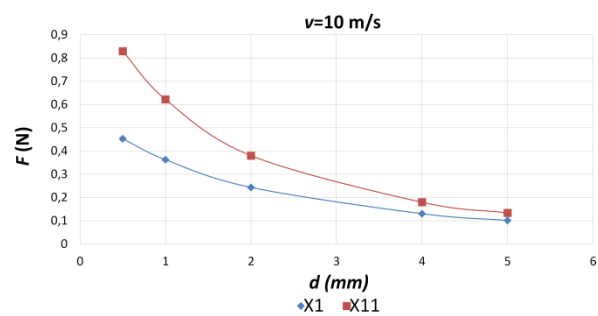


Figure 16. Variation of thrust force versus air gap width at rotor speed  $v=10$  m/s

The force values become higher as the air gap width decreases. Figures 12 to 18 show the variation of the forces with respect to the air gap width at various speeds for both X11 and X1 models.

At low speeds the decrease in percentages is not significant, but at high speeds, the percentage decrease in the force becomes very significant due to the decrease in the synchronous speed.

Another useful graphic is the one shown in Figure 20, which is the plot of the thrust force reduction in percentages with respect to the air gap width when the rotor speed is kept constant.

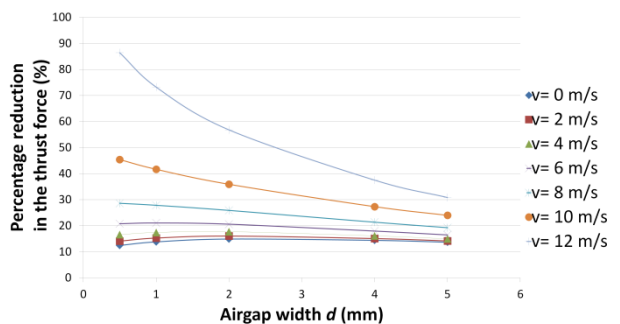


Figure 20. Percentage reduction of thrust force versus air gap width

In order to reduce the loss in the thrust force at high speeds, increasing the operation frequency seems to be the best simple solution, especially for narrower air gaps. The decrease in synchronous speed and the loss in the thrust force becomes very significant at high speeds (the speed range near the original synchronous speed calculated from the excitation frequency). So, increasing the frequency of the excitation may improve the operation at higher speeds especially for narrow air gaps. However, this may increase the iron losses. Not also that, whatever the speed and air gap width is, the loss is no less than about 12.4%.

## V. CONCLUSION

The goodness of a machine is defined by the goodness equation. This work suggests introducing an end effect factor to the goodness equation to take the dynamic longitudinal end effects into account.

FEM is a numerical method that is able to find magnetic field distribution of an electric motor. Linear induction motors have end effects and in order to calculate the influence of end effects, it is a good approach to build a reference motor model to compare. In this work, actual model is extended in both sides and an eleven times longer reference model called X11 model is built. While calculating the thrust force, only the rotor elements in the middle of X11 model are taken into calculation, which show no end effect contribution. These results are then compared with the ones of the actual end effect influenced X1 model. The results are sketched as  $F-v$  graphics to see and compare force variations with respect to the rotor speed.

The results show that the influences of end effects become very significant for narrower air gaps. This is because the rotor elements enter into and leave from a stronger magnetic field at both edges. The strength of the magnetic fields and the thrust force become larger for a narrower air gap. So, the zero thrust speed (synchronous speed) decreases, since the breaking effects of ends become significant.

As the rotor speed increases, the end effects become stronger in every case. All these results are as expected and agree with analytical calculations and reported experiments.

A narrower air gap means a higher *goodness* of a LIM. But especially at high speeds, it is lowered due to the end effects. So, it is possible to introduce an *end effect coefficient* to the goodness equation, which is a function of rotor speed in the case of LIM's.

All the results are obtained by means of a C program that uses finite element method written by the author. The force calculations are carried out by one of the three known methods. The excitation is taken as a current sheet of spatial sinusoidal distribution having sinusoidal variation in time, causing a traveling magnetic field. The magnitude of the excitation current is taken constant during all calculations.

## REFERENCES

- [1] A.H. Selcuk, H. Kurum, "Investigation of End Effects in Linear Induction Motors by Using the Finite Element Method", IEEE Transactions on Magnetics, Vol. 44, July 2008.
- [2] E.R. Laithwaithe, "Linear Electric Machines - A Personal View", Proceedings of IEEE, Vol. 63, No. 2, February 1975.
- [3] J.F. Gieras, G.E. Dawson, A.R. Eastham, "A New Longitudinal End Effect Factor for Linear Motors", IEEE Trans., Vol. 2, No. 1, pp. 152-159, 1987.
- [4] J.H. Sung, N. Kwanghee, "A New Approach to Vector Control for a Linear Induction Motor Considering End Effects", IEEE 34th IAS Annual Meeting, Vol. 4, pp. 2284-2289, Sep. 1999.
- [5] B.I. Kwon, K.I. Woo, S. Kim, "Finite Element Analysis of Direct Thrust Controlled Linear Induction Motor", IEEE Trans. on Mag., Vol. 35, No. 3, 1999.
- [6] N. Fujii, T. Harada, "Basic Consideration of End Effect Compensator of Linear Induction Motor for Transit", IEEE Conference Record, 2000.
- [7] D.K. Kim, B.I. Kwon, "A Novel Equivalent Circuit Model of Linear Induction Motor Based on Finite Element Analysis and its Coupling with External Circuits", IEEE Trans. Magn., Vol. 42, No. 10, pp. 3407-3409, Oct. 2006.
- [8] R. Haghmaram, A. Shoulaie, "Transient Modelling of Multi-Parallel Tubular Linear Induction Motors", IEEE Trans. Magn., Vol. 42, No. 6, pp. 1687-1693, June 2006.
- [9] K.A. Polzin, J.E. Adwar, A.K. Hallock, "Optimization of Electrodynamics Energy Transfer in Coilguns with Multiple, Uncoupled Stages", IEEE Trans. Magn., Vol. 49, No. 4, pp. 1453-1460, April 2013.
- [10] T. Morizane, K. Tsujikawa, N. Kimura, "Control of Traction and Levitation of Linear Induction Motor Driven by Power Source with Frequency Component Synchronous with the Motor Speed", IEEE Trans. Magn., Vol. 47, No. 10, Oct. 2011.
- [11] E. Amiri, E.A. Mendrela, "A Novel Equivalent Circuit Model of Linear Induction Motors Considering Static and Dynamic End Effects", IEEE Trans. Magn., Vol. 50, No. 3, March 2014.
- [12] S.M. Jang, et al., "Dynamic Characteristics of a Linear Induction Motor for Predicting Operating Performance of Magnetic Levitation Vehicles Based on Electromagnetic Field Theory", IEEE Trans. Magn., Vol. 47, No. 10, Oct. 2011.
- [13] Y. Zhang, et al., "A New Approach to Research the Transverse Edge Effect in Linear Induction Motor Considering the Edge Fringing Flux", IEEE Trans. Magn., Vol. 47, No. 11, Nov. 2011.
- [14] J.A. Duan, H.B. Zhou, N.P. Guo, "Electromagnetic Design of a Novel Linear Maglev Transportation Platform with Finite-Element Analysis", IEEE Trans. Magn., Vol. 47, No. 1, Jan. 2011.
- [15] P. Silvester, R.L. Ferrari, "Finite Elements for Electrical Engineers", Cambridge University Press, 1983.
- [16] A.H. Selcuk, "Investigation of End Effects in Linear Induction Motors by Using the Finite Element Method", Ph.D. Thesis, Firat University, Elazig, Turkey, 2003.

### **BIOGRAPHY**



**Ahmet Hakan Selcuk** was born in Turkey, 1968. He finished his B.Sc. degree at Department of Electrical and Electronics Engineering, Hacettepe University, Ankara, Turkey in 1990. He completed his M.Sc. degree at Department of Electrical and Electronics Engineering, Gaziantep

University, Gaziantep, Turkey in 1993, and finished his

Ph.D. degree at Department of Electrical and Electronics Engineering, Firat University, Elazig, Turkey in 2003. After three years at Gaziantep University as a research assistant, he became an instructor at Firat University in 1994. Then he started to work as Assistant Professor at Department of Electrical and Electronics Engineering, Balikesir University, Balikesir, Turkey since 2009. His M.Sc. thesis was on frequency selective surfaces, in the branch of microwaves and antennas and Ph.D. thesis was on investigation of end effects in linear induction motors by using FEM, in the branch of electrical machinery.